Thomas Jefferson University
Jefferson Digital Commons

Department of Biochemistry and Molecular Biology Faculty Papers

Department of Biochemistry and Molecular Biology

3-4-2022

Evidence for Paracrine Protective Role of Exogenous αA-Crystallin in Retinal Ganglion Cells

Madhu Nath
University of Michigan

Zachary B Sluzala
University of Michigan

Ashutosh S Phadte
Thomas Jefferson University

Yang Shan
University of Michigan

Angela M Myers
University of Michigan

Follow this and additional works at: https://jdc.jefferson.edu/bmpfp

Part of the Medical Biochemistry Commons, and the Medical Molecular Biology Commons

See next page for additional authors

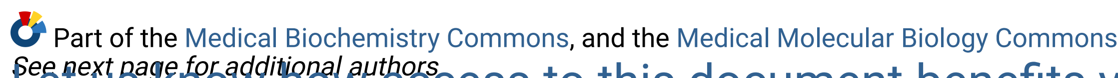

Recommended Citation

Nath, Madhu; Sluzala, Zachary B; Phadte, Ashutosh S; Shan, Yang; Myers, Angela M; and Fort, Patrice E, "Evidence for Paracrine Protective Role of Exogenous αA-Crystallin in Retinal Ganglion Cells" (2022). *Department of Biochemistry and Molecular Biology Faculty Papers.* Paper 210.
https://jdc.jefferson.edu/bmpfp/210

This Article is brought to you for free and open access by the Jefferson Digital Commons. The Jefferson Digital Commons is a service of Thomas Jefferson University's Center for Teaching and Learning (CTL). The Commons is a showcase for Jefferson books and journals, peer-reviewed scholarly publications, unique historical collections from the University archives, and teaching tools. The Jefferson Digital Commons allows researchers and interested readers anywhere in the world to learn about and keep up to date with Jefferson scholarship. This article has been accepted for inclusion in Department of Biochemistry and Molecular Biology Faculty Papers by an authorized administrator of the Jefferson Digital Commons. For more information, please contact: JeffersonDigitalCommons@jefferson.edu.

Authors
Madhu Nath, Zachary B Sluzala, Ashutosh S Phadte, Yang Shan, Angela M Myers, and Patrice E Fort

This article is available at Jefferson Digital Commons: https://jdc.jefferson.edu/bmpfp/210

eNeuro Accepted Manuscript

eNeuro

Research Article: New Research | Disorders of the Nervous System

Evidence for Paracrine Protective Role of Exogenous αA-Crystallin in Retinal Ganglion Cells

https://doi.org/10.1523/ENEURO.0045-22.2022

Cite as: eNeuro 2022; 10.1523/ENEURO.0045-22.2022

Received: 28 January 2022
Accepted: 2 February 2022

This Early Release article has been peer-reviewed and accepted, but has not been through the composition and copyediting processes. The final version may differ slightly in style or formatting and will contain links to any extended data.

Alerts: Sign up at www.eneuro.org/alerts to receive customized email alerts when the fully formatted version of this article is published.

Copyright © 2022 Nath et al.
This is an open-access article distributed under the terms of the Creative Commons Attribution 4.0 International license, which permits unrestricted use, distribution and reproduction in any medium provided that the original work is properly attributed.

eNeuro Accepted Manuscript

Evidence for Paracrine Protective Role of Exogenous αA-Crystallin in Retinal Ganglion Cells

1. *Exogenous αA-crystallin in retinal neuroprotection*

2. Madhu Nath[1*], Zachary B. Sluzala[1*], Ashutosh S. Phadte[1,2*], Yang Shan[1], Angela M. Myers[1], and Patrice E Fort[1,3]

[1]Department of Ophthalmology and Visual Sciences, University of Michigan, Ann Arbor, Michigan, USA. [2]Currently in Department of Biochemistry and Molecular Biology, Thomas Jefferson University, Philadelphia, Pennsylvania, [3]Department of Molecular and Integrative Physiology, University of Michigan, Ann Arbor, Michigan, USA.

*These authors should be viewed as equal contributors and co-first authors.

3. Designed research, PEF; Performed research, MN, AP, ZBS, YS and AM; Contributed unpublished reagents/ analytic tools, PEF and AM; Analyzed data, PEF, MN, AP, ZBS, YS and AM; Wrote the paper, PEF, MN, AP, ZBS, YS and AM.

4. **Corresponding Author:** Dr. Patrice E Fort
   Associate Professor,
   Department of Ophthalmology & Visual Sciences, and Department of Molecular and Integrative Physiology, The University of Michigan, Ann Arbor, Michigan Email-patricef@umich.edu

5. **Number of Figures:** 7
6. **Number of Tables:** 1
7. **Number of Multimedia:** 0
8. Abstract-229
9. Significance statement - 120
10. Introduction- 891
11. Discussion- 1380

12. Acknowledgement: This research was performed in part supported by Research to Prevent Blindness (RPB).
13. **Conflicts of Interest:** Dr. Fort has intellectual property interests and is listed as inventor on a patent for the use of CryAA as a retinal neuroprotective treatment. The other authors declare no conflict of interest.
14. This research was supported by National Eye Institute (EY020895), NIH P30EY007003 (Core Grant for Vision Research at the University of Michigan), and NIH P30DK020572 (Michigan Diabetes Research Center) as well as the Lichter Award.

eNeuro Accepted Manuscript

38

39

40 **Evidence for Paracrine Protective Role of Exogenous αA-Crystallin in Retinal**
41 **Ganglion Cells**

42

43

44 **Keywords:** αA-Crystallins; Recombinant Proteins; Chaperone; Neuroprotection; Metabolic
45 Stress

46

eNeuro Accepted Manuscript

Abstract:

Expression and secretion of neurotrophic factors have long been known as a key mechanism of neuroglial interaction in the central nervous system. In addition, several other intrinsic neuroprotective pathways have been described, including those involving small heat shock proteins such as α-crystallins. While initially considered as a purely intracellular mechanism, both αA- and αB-crystallins have been recently reported to be secreted by glial cells. While an anti-apoptotic effect of such secreted αA-crystallin has been suggested, its regulation and protective potential remain unclear. We recently identified residue T148 and its phosphorylation as a critical regulator of αA-crystallin intrinsic neuroprotective function. In the current study, we explored how mutation of this residue affected αA-crystallin chaperone function, secretion, and paracrine protective function using primary glial and neuronal cells. After demonstrating the paracrine protective effect of αA-crystallins secreted by primary Müller glial cells, we purified and characterized recombinant αA-crystallin proteins mutated on the T148 regulatory residue. Characterization of the biochemical properties of these mutants revealed an increased chaperone activity of the phosphomimetic T148D mutant. Consistent with this observation, we also show that exogeneous supplementation of the phosphomimetic T148D mutant protein protected primary retinal neurons from metabolic stress despite similar cellular uptake. In contrast, the non-phosphorylatable mutant was completely ineffective.

Altogether, our study demonstrates the paracrine role of αA-crystallin in the central nervous system as well as the therapeutic potential of functionally enhanced αA-crystallin recombinant proteins to prevent metabolic-stress induced neurodegeneration.

Significance statement

αA-crystallin is a chaperone protein that has been long known for its critical role in the lens proteostasis. Recent studies have highlighted the protective potential of αA-crystallin in the central nervous system, especially the retina. The broad chaperone and cytoprotective functions of αA-crystallin make it a very attractive target in the context of the dire need for novel protective therapies for neurodegenerative diseases. Our previous work has shown that phosphorylation on threonine 148 (T148) is a critical regulator of the cytoprotective function of αA-crystallin. The current study demonstrates that αA-crystallin secreted by Müller glial cells plays a paracrine protective role for retinal neurons. We further demonstrated the therapeutic potential of a functionally enhanced αA-crystallin recombinant protein in promoting neuronal survival.

eNeuro Accepted Manuscript

80 **Introduction**

81 α-Crystallins (αA- and αB-) have been extensively described as resident chaperone proteins in
82 the eye lens and are imperative for maintaining transparency (Ghosh and Chauhan, 2019;
83 Hejtmancik et al., 2015; Makley et al., 2015; Masilamoni et al., 2005). In recent years, both
84 proteins gained substantial interest in the context of retinal insults and neurodegenerative
85 diseases (Munemasa et al., 2009; Piri et al., 2013; Wang et al., 2011; Ying et al., 2008; Zhu and
86 Reiser, 2018). Although the presence of α-crystallins was initially described and studied in the
87 ocular lens, their expression is not limited to this tissue. αB-crystallin is ubiquitously expressed
88 or stress-induced in most tissues and cells, including heart, skeletal muscle, kidney, lung, brain,
89 and retina. αA-crystallin, however, is basally expressed at low levels in a limited number of
90 tissues while highly induced under stress conditions in the kidney and the central nervous
91 system, including the retina (Dubin et al., 1991; Zhang et al., 2019). In the retina, both α-
92 crystallin proteins have been found predominantly in glia and retinal ganglion cells (RGCs) in
93 the inner retina, as well as photoreceptors and retinal pigmental epithelium (RPE) in the outer
94 retina (Kannan et al., 2016; Kase et al., 2012; Munemasa *et al.*, 2009; Rao et al., 2008;
95 Ruebsam et al., 2018; Shi et al., 2015). Initially thought to be products of gene duplication, both
96 αA- and αB-crystallins are now known to present different expression patterns and functional
97 roles, independent from each other, including in neuroprotection (Robinson and Overbeek,
98 1996).

99 The neuroprotective function has been recently linked to both αA- and αB-crystallins in the
100 context of different neurodegenerative diseases (Kannan *et al.*, 2016; Zhu and Reiser, 2018).
101 Proposed mechanisms for these neuroprotective functions of α-crystallin proteins include
102 attenuation of mitochondrial dysfunction (Zhu and Reiser, 2018), reduced accumulation of
103 misfolded proteins (Schmidt et al., 2012) and specific disruption of neuronal apoptotic pathways
104 (Hua Wang et al., 2020; Piri *et al.*, 2013; Piri et al., 2016). Additionally, studies have established

eNeuro Accepted Manuscript

105 a strong relationship between these two protein's expression and chaperone activity and their
106 observed anti-apoptotic function (Pasupuleti et al., 2010; Piri *et al.*, 2013). As members of the
107 small heat shock protein family, α-crystallins have been shown to prevent protein aggregation
108 as well as promote cell survival under conditions such as chemically induced hypoxia (Schmidt
109 *et al.*, 2012; Yaung et al., 2008) including through inhibition of apoptosis. Expression of αA- and
110 αB-crystallins have been shown to increase in an experimental model of light-induced damage
111 to the retina (Heinig et al., 2020), as well as at different stages of the wound healing process
112 following retinal tear (Baba et al., 2015). Consistent with a protective potential for retinal
113 neurons, α-crystallin expression was also shown to correlate with increased RGC survival
114 following optic nerve axotomy (Munemasa *et al.*, 2009) and in rescuing photoreceptors in a
115 light-induced damage model (Heinig *et al.*, 2020).

116 Studies from our lab and others have reported an increased αA-crystallin expression in the
117 retinas of diabetic rodents as well as human donors with diabetes (Fort et al., 2009; Ruebsam *et*
118 *al.*, 2018). However, αA-crystallin function seemed to be impaired in the diabetic retina, as
119 suggested by loss of solubility, and change in their post-translational modification (PTM) pattern
120 (Reddy et al., 2013). PTMs have been reported to not only influence the structure but also the
121 neuroprotective and chaperone functions of α-crystallins (Heise et al., 2013; Kim et al., 2007).
122 Specifically, phosphorylation on serine residues 19, 45, and 59 of αB-crystallin (Heise *et al.*,
123 2013; Kim *et al.*, 2007; Reddy *et al.*, 2013) and residue 122 and 148 of αA-crystallin seem to be
124 critical regulators of their chaperone and protective functions (Ruebsam *et al.*, 2018).
125 Interestingly, while previous studies have shown increased phosphorylation for αB-crystallin
126 (Heise *et al.*, 2013; Reddy *et al.*, 2013), αA-crystallin phosphorylation on residue 148 was
127 dramatically reduced in the retina from diabetic rodents and diabetic donors, especially those
128 with retinopathy (Ruebsam *et al.*, 2018). We also showed that the T148D phosphomimetic form
129 of αA-crystallin is a potent neuroprotector for retinal neurons against serum deprivation-induced

eNeuro Accepted Manuscript

130 cell death (Ruebsam *et al.*, 2018). Furthermore, we have demonstrated that glial cells
131 overexpressing αA-crystallin secrete the protein in their extracellular environment and that
132 supplementation of conditioned media from these cells efficiently promotes R28 cell survival
133 following exposure to serum starvation-induced apoptotic stress (Ruebsam *et al.*, 2018).
134 Interestingly, these observed anti-apoptotic effects were only observed from cells expressing
135 the wild-type or phosphomimetic (T148D) protein, but not its non-phosphorylatable counterpart
136 (T148A). While this pointed to a critical role of this phosphorylation, the impact of this post-
137 translational modification on the structure-function relationship of αA-crystallin remains
138 unknown.

139 In all, our current understanding of α-crystallin function draws out two major observations that 1)
140 αA-crystallin serves a key neuroprotective function within the retinal tissue and 2)
141 controlling/enhancing αA-crystallin function presents the high potential to promote retinal cell
142 survival and maintenance of the microarchitecture of the neuroretina. Therefore, in the present
143 study, we studied the impact of T148D mutation of αA-crystallin on its chaperone function and
144 associated alteration of its biochemical properties. Furthermore, we assessed the potential of
145 supplementation with recombinant T148D αA-crystallin protein to promote survival of retinal
146 neurons, especially primary RGCs, following exposure to metabolic stress. The current study,
147 therefore, unveils an exciting new avenue for the use of αA-crystallin and its functionally
148 enhanced derivatives to slow the progression of retinal neurodegenerative disorders.

149

150 **Methods**

151 ***Cell lines.*** Rat retinal Müller cells (rMC-1) and retinal neuronal cell (R28) lines were obtained
152 from Applied Biological Materials Inc. (Richmond, BC, Canada). All cell lines were maintained in
153 DMEM, 5 mM Glucose (DMEM-NG) supplemented with 10 % FBS (Flow Laboratories) at 37 °C,

eNeuro Accepted Manuscript

154 5 % CO_2 unless stated otherwise. For experiments, R28 cells were differentiated into neurons in
155 DMEM with 8-(4-Chlorophenylthio) adenosine 3′,5′-cyclic monophosphate (8-CPT-cAMP,
156 Catalogue # C3912, Millipore Sigma, St. Louis, MO) at a final concentration of 2.5 mM on
157 laminin-coated plates as described earlier (Ruebsam *et al.*, 2018).

158 **Primary Müller glial cells (MGCs)** were obtained from the αA-crystallin knockout mice
159 originally generously provided by Dr. Wawrousek from the National Eye Institute (NEI). Cells
160 were isolated using a protocol adapted from Hicks and Courtois (Hicks and Courtois, 1990) and
161 characterized previously (Brady et al., 1997). Briefly, primary MGCs were isolated from the
162 retinal tissue of P10-14 αA-crystallin knockout mice pups and maintained in DMEM-NG + 10%
163 FBS + 1% Penicillin/Streptomycin (Catalogue # 15140122, Thermo Fisher Scientific, Waltham,
164 MA). The purity and specificity of the cell preparation were validated by evaluating the
165 expression of the Müller cell-specific markers glutamine synthetase, Prdx-6, and Abc8a from
166 Passage 2-6 as described previously (Nath et al., 2021).

167 **Primary retinal ganglion cells (RGCs).** RGCs were isolated and purified from αA-crystallin
168 knockout mice pups at P3-P5 using a modified immunopanning method described previously
169 (Winzeler and Wang, 2013). The purified RGCs were resuspended in growth media containing
170 B27 supplement (Thermo Fisher), 50 ng/ml BDNF (Catalogue # B3795, Millipore Sigma, St.
171 Louis, MO), 10 ng/ml CNTF (Catalogue # C3835, Millipore Sigma, St. Louis, MO) and 4 µg/ml
172 forskolin (Catalogue # F3917, Millipore Sigma, St. Louis, MO) before being seeded onto poly-D-
173 lysine and laminin-coated glass coverslips in 24-well culture plates. Cells were seeded at a
174 density of 30,000 cells/$cm^{2,}$ and the growth media was changed every three days until use.

175 ***Transient transfection of rMC-1 and MGCs and recovery of conditioned media.*** Cells were
176 transfected using the Neon Transfection System (Invitrogen) following the manufacturer's
177 instructions. Briefly, cells were trypsinized and washed in PBS before being resuspended in 110
178 µl resuspension buffer and electroporated with 2.5 µg of the previously characterized pcDNA

eNeuro Accepted Manuscript

179 3.1 vectors expressing either WT, the phosphomimetic T148D, or the non-phosphorylatable
180 T148A crystallins, respectively (Ruebsam *et al.*, 2018) and were seeded in 6-well plates. The
181 next day, transfected cells were incubated either in serum-free DMEM-NG (with 20mM
182 Mannitol), DMEM-HG (DMEM-NG with 20 mM glucose), or DMEM-HG with 100ng/ml TNFα
183 (Catalogue # 210-TA, R&D systems, Minneapolis, MN) for 24 hours. Cells incubated in DMEM-
184 NG served as the experimental control.

185 Following incubation, growth media from transfected glial cells was recovered and prepared as
186 previously described (Ruebsam *et al.*, 2018). Briefly, the media was first filtered using a 0.22 μm
187 syringe filter (Catalogue #, Millipore Sigma, St. Louis, MO) and then centrifuged sequentially at
188 300 × g for 6 minutes, 3,000 × g for 20 minutes, and 5,000 × g for 10 minutes at room
189 temperature. Finally, the media were concentrated using 3K MWCO concentrators (Catalogue #
190 C775, Amicon, Merck Millipore, USA) and stored at 4 °C until use in conditioned media
191 experiments.

192 **Generation of recombinant αA-crystallins.** pET23d+ vectors containing the cDNA sequence
193 for human αA-crystallin were used as a template for generating mutant proteins. Point mutations
194 on T148 corresponding to the phosphomimetic (T148D) and the non-phosphorylatable (T148A)
195 analogue of αA-crystallin were introduced using the Quikchange Site-directed mutagenesis kit
196 (Agilent Technologies, Santa Clara, CA) using primers listed in table 1. Cloned plasmids were
197 scaled up in XL-1 Blue supercompetent cells, and isolated plasmid sequences were confirmed
198 by Sanger sequencing. Sequenced plasmids were then used to transform BL21(DE3) pLysS
199 cells to optimize the respective proteins' expression.

200 Cells were grown in LB Miller broth (Catalogue # BP142610P1, Fisher Scientific) in a rotary
201 shaker maintained at 37 °C, 225 rpm, till they reached an OD_{600} between 0.4-0.6. Protein
202 expression was induced by the addition of isopropyl-β-D-thioglalctopyranoside (IPTG,
203 Catalogue # I2481C, GoldBio, St. Louis, MO) at a final concentration of 500 μM for 4 hours.

eNeuro Accepted Manuscript

204 Bacterial cell pellets were harvested by centrifugation at 4000 rpm for 20 minutes at 4 °C and
205 stored overnight at - 80 °C. Cell Lysis and protein purification was carried out using size
206 exclusion chromatography as described in (Horwitz et al., 1999). Purified proteins were
207 subjected to endotoxin removal using Triton X-114 mediated phase separation using a protocol
208 adapted from (Teodorowicz et al., 2017). The efficacy of endotoxin removal was ascertained
209 using the Pierce™ Chromogenic Endotoxin Quant Kit (Catalogue # A39552, Thermo Fisher
210 Scientific, Waltham, MA) as per manufacturer's instructions. Protein purity was assessed by
211 Coomassie blue staining and Immunoblot analysis (Figure 3A). All proteins were stored in PBS
212 pH 7.4 at – 80 °C until use.

213 **Chaperone activity assay.** The functional efficacy of purified αA-crystallins to prevent non-
214 specific protein aggregation *in vitro* was assessed by chaperone assays as described previously
215 (Horwitz, 1992). Aggregation of 75 µg alcohol dehydrogenase (ADH) in PBS pH 7.4 against
216 varied amounts of αA-crystallin was chemically induced by adding EDTA at a concentration of
217 37.5 mM. Protein aggregation was monitored as relative absorbance at 360 nm in a FLUOstar
218 OMEGA plate reader (BMG Labtech). Representative assays are an average of three
219 independent experiments for statistical significance.

220 **Native gel electrophoresis.** The polydispersity profile of purified αA-crystallins *in vitro* was
221 assessed by Native PAGE gels. Samples were prepared using 7.5 µg of recombinant WT,
222 T148D or T148A αA-crystallin resuspended in Novex™ Tris-Glycine Native Sample Buffer (2X)
223 (Catalogue # LC2673, Thermo Fisher Scientific) and deionized water. Samples were loaded on
224 NativePAGE™ 3 to 12%, Bis-Tris gels (Catalogue # BN1001BOX, Thermo Fisher Scientific).
225 Gels were run using 1X NativePAGE™ Anode Buffer and 1X NativePAGE™ Dark Blue Cathode
226 Buffer as per manufacturer's instructions. Gels were fixed and de-stained as per manufacturer's
227 instructions and then imaged using a FluorChem™ E system (Protein Simple). Images were
228 analyzed using the Gel Analyzer function of ImageJ (Schneider et al., 2012) and the molecular

eNeuro Accepted Manuscript

229 size markers run on either side of the recombinant proteins, allowing us to obtain the median
230 size of the oligomers for each recombinant protein. The area under the curve is shown as a
231 function of oligomer sizes from less than 480 to 1236 kDa, with the median shown for each
232 recombinant protein.

233 **Solubility assays**. As above, cells were transfected with 2.5 µg of pcDNA 3.1(+) plasmids
234 expressing either WT, T148D, or T148A crystallins or an empty vector (EV) and were seeded in
235 6-well plates. The next day, transfected cells were incubated either in DMEM-NG + 10% FBS or
236 serum-free DMEM-NG for 4 or 24 hours. Cells transfected with EV served as an experimental
237 control. Following incubation, cells were harvested on ice in chilled RIPA buffer (100mM Tris pH
238 7.5, 3mM EGTA, 5mM MgCl2, 0.5% Triton X-100, 1mM PMSF, 1X complete EDTA-free
239 protease inhibitor cocktail tablet (Roche Diagnostics, Indianapolis, IN)) and subjected to
240 immunoblot analyses.

241 **Protein uptake assay.** Differentiated R28 cells were allowed to grow on laminin-coated plates
242 for 36 hours. Recombinant WT, T148D, or T148A crystallins were supplemented to growth
243 media at a concentration of 500 ng/ml. Protein uptake in R28 cells was tested in DMEM-NG
244 versus serum-free DMEM-NG, the presence and absence of BSA for 4 hours. Protein uptake by
245 R28 cells was also tested under stress by incubating cells in serum-free DMEM-NG (with 20mM
246 Mannitol), DMEM-HG (DMEM-NG with 20 mM glucose), or DMEM-HG with 100ng/ml TNFα.
247 Following incubation, cells were harvested on ice in chilled RIPA buffer and subjected to
248 immunoblot analyses.

249 **Proteinase K susceptibility assay.** Differentiated R28 cells were allowed to grow on laminin-
250 coated 6-well plates for 36 hours. Recombinant WT αA-crystallin was supplemented with growth
251 media at a 500 ng/ml concentration for 2, 4, and 24 hours. The cell lysates were then subjected
252 to proteinase K treatment as adopted by Ruebsam et al.,2018. Briefly, cell lysates were treated
253 with 100 ng proteinase K (Millipore Sigma) in a reaction containing 10 mM Tris-HCl (pH 7.4)

eNeuro Accepted Manuscript

254 with or without Triton X-100 (1%) for 30 minutes at 37°C. The reaction was stopped by the
255 addition of loading buffer and heated at 70°C for 10 minutes. A control sample was treated the
256 same way, aside from the omission of the enzymes. Protein levels were then assessed by
257 immunoblotting as described below.
258
259 **Immunoblotting Analyses.** Protein concentrations were measured with the Pierce BCA
260 reagent, and all samples and conditioned media were adjusted for equal protein concentration.
261 To assess the purity of the recombinant protein preparations, 50 ng of pure protein was
262 subjected to immunoblot analyses. For protein uptake experiments, cells were homogenized by
263 sonication in RIPA buffer as described previously (Ruebsam *et al.*, 2018) and 35 µg of the total
264 cell lysate was loaded on 4-12% NuPage Bis-Tris gels (Thermo Fisher). Gels were run in MES
265 buffer (Thermo Fisher Scientific) as per manufacturer's instructions. Western blot transfer was
266 carried out on nitrocellulose membranes using the Mini Trans-Blot cell (Catalogue # 1703930,
267 Bio-Rad) at 160 V for 1 hour at 4 °C. For solubility assays, RIPA-soluble protein lysates were
268 collected, and insoluble pellets were resuspended after PBS wash by sonication in Urea buffer
269 (10mM Tris pH 7.5, 150mM NaCl, 5mM EGTA, 5mM $MgCl_2$, 1mM DTT, 0.1% Triton X-100,
270 0.2mM PMSF, 9M Urea). Soluble samples were adjusted for equal protein concentration, while
271 insoluble samples were adjusted for equal volume. Samples were loaded on 4-12% NuPage
272 Bis-Tris gels and run in MES buffer as per manufacturer's instructions, at 110 V. Cell lysates
273 and conditioned media were immunoblotted for αA-crystallin (sc-28306, Santacruz
274 Biotechnology, Dallas, TX) and β-actin (MAB-1501, Millipore) as a loading control. Solubility was
275 measured as a ratio of insoluble αA-crystallin to total αA-crystallin for each condition (using the
276 Gel Analyzer function in ImageJ (Schneider *et al.*, 2012), normalized to WT, and data were
277 analyzed using the GraphPad Prism software module (GraphPad Software, San Diego, CA).

eNeuro Accepted Manuscript

278 **Cell death Assay.** Cell death rates were assessed by DNA Fragmentation ELISA or TUNEL
279 staining. For the DNA fragmentation ELISA (Roche Diagnostics, Indianapolis, IN), R28 cells
280 were seeded in a 96 well plate at a density of $1{\times}10^5$ cells per well and incubated with 100 µl of
281 conditioned medium for 4 hours before being processed according to the manufacturer's
282 instructions and as previously described (Ruebsam *et al.*, 2018). The colorimetric signal was
283 measured with a fluorescence plate reader in a FLUOstar OMEGA plate reader (BMG Labtech)
284 with excitation at 405 and 490 nm.

285 For TUNEL staining, cells were seeded on glass coverslips as previously described. Following
286 incubation, the coverslips were fixed in 4% PFA and stained for TUNEL (DeadEnd™
287 Fluorometric TUNEL System, Promega) according to manufacturer's instructions. Briefly, the
288 samples were incubated with fluorescent-labeled dUTP and TdT enzymes. The nuclei were
289 visualized by Hoechst staining. Images were captured on a Leica DM6000 fluorescent
290 microscope. Nuclei and TUNEL positive cells were counted using ImageJ (Schneider *et al.*,
291 2012) and data were analyzed using the GraphPad Prism software module (GraphPad
292 Software, San Diego, CA).

293 For primary RGC, characterization of the primary cells was performed by immunostaining with
294 RGC specific markers – β3-tubulin (Biolegend, Catalogue #801201), Neurofilament-H (NF-H,
295 Millipore, Catalogue #NE1023), and RNA-binding protein with multiple splicing (RBPMS,
296 (Rodriguez et al., 2014), Genetex, Catalogue #GTX118169). For cell survival experiments, the
297 coverslips were first subjected to TUNEL staining as described above. After TUNEL, the
298 coverslips were immunostained with RBPMS antibody and secondary Alexa Flour 594 labeled
299 antibody (Invitrogen, A21207). All Immunostainings were visualized, and images were captured
300 using Leica DM6000 fluorescent microscope. Cells staining positive for RBPMS and both
301 TUNEL and RBPMS were counted using the Imaris software module (Bitplane AG, Zurich,

eNeuro Accepted Manuscript

302 Switzerland). The data were analyzed using GraphPad Prism (GraphPad Software, San Diego,
303 CA).

304 **Statistics:**

305 For immunoblot experiments, the data were normalized to the housekeeping signal as a control
306 before analysis. ANOVA models with heterogeneous variances, adjusted for the replication of
307 the experiment, were fit to the data to assess differences between test and control group.
308 Analyses were performed using nonrepeated-measures ANOVA, followed by the Tukey post-
309 hoc tests for multiple comparisons, whereas 2-tailed t test was used for a single comparison.
310 A P value less than 0.05 was considered significant.

311

312 **Results:**

313 **Expression and secretion of αA-crystallin in MGCs.** Müller glial cells (MGCs) are
314 instrumental in maintaining neuronal homeostasis in the retina, with defined functions ranging
315 from the recycling of neurotransmitters to controlling ionic and water equilibrium (Dulle and Fort,
316 2016). Our previous work emphasized the upregulation of αA-crystallin in the glia and ganglion
317 cell layers of retinal tissue from human donors with diabetes compared to non-diabetic controls.
318 Furthermore, growth media from rMC-1 cells overexpressing αA-crystallin efficiently promoted
319 survival of R28 cells under serum starvation-induced apoptotic stress (Ruebsam *et al.*, 2018).
320 To further investigate the role of αA-crystallin in MGCs, we compared the relative expression of
321 αA-crystallin in rMC-1 and primary Müller glial cells isolated from αA-crystallin knockout mice.
322 Cells from αA-crystallin knockout mice were used throughout this study to avoid potential
323 confounding effect of endogenously expressed and induced WT αA-crystallin. Thus, cells
324 lacking endogenous αA-crystallin expression were transfected with either empty vectors or
325 vectors driving expression of the wild-type protein (WT), the functionally enhanced

eNeuro Accepted Manuscript

326 phosphomimetic (T148D), or the non-phosphorylatable (T148A) analogue, and αA-crystallin
327 expression was verified by immunoblot.

328 As we previously reported, WT, 148A, and 148D αA-crystallin expressed well in transfected
329 rMC-1. We also observed corresponding levels of secreted proteins in the cell culture media
330 (conditioned media, **Figure 1A, left panel**). Additionally, the expression of all three crystallin
331 constructs was consistent in the cell lysate and conditioned media under normal conditions as
332 well as under conditions of metabolic and "diabetes-like" stress (**Figure 1A, middle and right**
333 **panel**). Importantly, we also report that primary MGCs could be transfected with the same
334 vectors, leading to expression levels and secretion comparable to those seen in rMC-1 (**Figure**
335 **1B**). Similar to rMC-1, our data also clearly show that stress exposure does not affect the
336 expression and secretion of any of our αA-crystallin constructs.

337 **Neuroprotective potential of MGC secreted αA-crystallin.** Overexpression of αA-crystallin in
338 multiple cell models has demonstrated its anti-apoptotic potential under conditions of stress-
339 induced cell death (Christopher et al., 2014; Liu et al., 2004; Losiewicz and Fort, 2011;
340 Pasupuleti *et al.*, 2010; Ruebsam *et al.*, 2018). To investigate the protective potential of MGC
341 secreted αA-crystallin, we tested the effect of conditioned media obtained from αA-crystallin
342 transfected primary MGCs on retinal neurons subjected to metabolic stress. Supplementation of
343 conditioned media from MGCs overexpressing WT and T148D crystallin highly promoted R28
344 cell survival under serum starvation-induced metabolic stress, as evidenced by the reduction in
345 cell death by 45% and 37%, respectively. Similarly, in "diabetes-like" stress, conditioned media
346 from MGCs overexpressing WT or 148D αA-crystallin resulted in 38% and 44% reduction in
347 R28 cell death, respectively. Supportive of the key role of T148 phosphorylation, media from
348 T148A overexpressing MGCs was ineffective in promoting R-28 cell survival in either stress
349 (**Figure 2A and B**). Immunoblot analysis of the cell lysate and conditioned media confirmed that
350 this difference in protective effect was not due to lower levels of expression or secretion of

eNeuro Accepted Manuscript

351 T148A (**Figures 2C and D**). We then tested the effect of conditioned media on primary, αA-
352 crystallin knockout (AKO) mouse RGCs. As in R28 cells, supplementation of conditioned media
353 from MGCs overexpressing WT and T148D crystallin highly promoted RGC survival under
354 "diabetes-like" stress, while media from T148A overexpressing MGCs did not (**Figure 2E**).
355 Taken together, these data clearly demonstrate the neuroprotective potential of αA-crystallin
356 and validate a paracrine role of MGC secreted αA-crystallin in promoting neuronal cell survival
357 under stress.

358 **Characterization of recombinant αA-crystallins.** Our experiments with secreted αA-crystallin
359 highlighted the neuroprotective potential of extracellular WT and T148D crystallins in promoting
360 neuronal cell survival exposed to serum starvation and "diabetes-like" conditions. This prompted
361 us to assess if our observation from the conditioned media experiments could be recapitulated
362 using purified, recombinant αA-crystallin proteins. All three proteins, WT, T148A, and T148D
363 were scaled up from BL21(DE3) pLysS cells expressing the specified constructs and purified by
364 size exclusion chromatography. As shown in **Figure 3A**, the three purified proteins show a high
365 degree of purity, as validated by SDS-PAGE and immunoblotting analyses. Because
366 recombinant proteins purified from bacterial sources are often contaminated with bacterial
367 endotoxins, which compromises their use *in vivo*, our protein preparations were treated with
368 Triton X-114, a treatment routinely used to promote efficient endotoxin removal (Teodorowicz *et*
369 *al.*, 2017). Qualitative analysis of the recombinant protein preparations post Triton X-114
370 mediated phase separation confirmed the more than 90% reduction in the total endotoxin
371 content (**Figure 3B**).

372 αA-crystallins were initially characterized in the eye lens as chaperone proteins, efficiently
373 preventing non-specific protein aggregation and promoting organ transparency. *In vitro*, we
374 tested the relative chaperone function of WT, T148D, and T148A crystallins by employing
375 aggregation kinetics assays. As previously shown, EDTA-induced aggregation of ADH was

eNeuro Accepted Manuscript

376 suppressed by αA-crystallins in a concentration-dependent manner (**Figure 3C**). Consistent with
377 enhancing αA-crystallin chaperone activity by its phosphorylation on T148, the T148D mutant
378 was significantly more effective at preventing ADH aggregation *in vitro* (**Figure 3D**). While the
379 WT αA-crystallin exhibited an IC50 of 8 µg, that of the T148D crystallin mutant was 4.4 µg,
380 demonstrating an increase in chaperone efficacy of 45 percent. The phosphorylation of αA-
381 crystallin on T148, therefore, results in an enhancement of its chaperone function.

382 **Stress-induced insolubility of αA-crystallin.** WT, T148D, and T148A αA-crystallin expressed
383 in R28 cells exhibited no differences in basal solubility (**Figure 4A**). However, following 4 hours
384 of serum starvation, T148A trended towards higher insolubility, and T148D trended toward lower
385 insolubility (data not shown), an effect confirmed and enhanced after 24 hours of serum
386 starvation (**Figure 4B**). This observation indicates that phosphorylation on residue T148 plays a
387 key role in promoting αA-crystallin's function, including by reducing stress-induced insolubility.

388 **T148 phosphorylation-dependent changes in oligomer size.** αA-crystallin, along with its
389 close relative αB-crystallin is known to exist as larger oligomers, we thus assessed how this
390 phosphorylation impacts the oligomeric state of αA-crystallin. T148A αA-crystallin formed
391 slightly larger oligomers (median 669 kDa) than the WT αA-crystallin (median 650 kDa),
392 whereas T148D formed substantially smaller oligomers (median 613 kDa; Figure 4C-D). This
393 data is clearly supportive of the T148 phosphorylation state impacting oligomeric and potentially
394 aggregate formation. This could also partially explain the solubility data as the decreased
395 oligomeric size observed for the T148D mutant could promote the protein's solubility under
396 stress conditions. Together the solubility and oligomeric data are consistent with the relative
397 pro-survival potential of the mutants. As αA-crystallin becomes more insoluble and/or forms
398 larger oligomers, less is likely available to serve normal chaperone and protective roles.

eNeuro Accepted Manuscript

399 **Uptake of recombinant αA-crystallins.** Our previous study showed that conditioned media
400 from MGCs expressing αA-crystallins WT and T148D greatly reduced stress-induced R28 cell
401 death. Prior to testing the neuroprotective efficacy of the different recombinant αA-crystallins, we
402 first characterized the specificity of their uptake in R28 cells. As expected, supplementation of
403 recombinant αA-crystallins to differentiated R28 cells showed a gradual increase in their uptake
404 as a function of time (**Figure 5A**). We then assessed the impact of stress on protein uptake and
405 showed that serum starvation was associated with an increased uptake of all recombinant
406 proteins, including T148A, although slightly less than WT and T148D αA-crystallins. Since
407 T148A is taken up by the cells under stress, it can be asserted that the level of protein uptake is
408 not solely responsible for the relative protective efficacy of the different recombinant proteins.

409 To eliminate the possibility that the increased uptake of recombinant proteins observed in serum
410 starvation is facilitated by the lack of interactions that would otherwise occur with components of
411 FBS, we spiked the growth media with saturating concentrations of BSA (1%). Supplementation
412 of BSA did not impact protein uptake, suggesting the difference in uptake of proteins as part of
413 the stress response (**Figure 5B**). The level of protein uptake was further investigated by
414 characterizing protein uptake under "diabetes-like" conditions (**Figure 5C**). Protein uptake
415 progressively increased in cells exposed to "diabetes-like" conditions (HG, HG+TNFα lanes)
416 and is independent of T148 mutation (**Figure 5C**). Collectively, our data demonstrate that T148
417 mutation does not dramatically impact its uptake by R28 cells in a way that could significantly
418 affect its observed neuroprotective efficacy under stress.

419 Following the uptake assay of recombinant proteins, the R28 cells were further assessed for the
420 internalization of these proteins. The obtained results have demonstrated the time-dependent
421 marked expression of recombinant WT αA-crystallin in R-28 cells in the intact cell membrane
422 during protease digestion. On the contrary, the intracellular access of protease in R-28 cells led

eNeuro Accepted Manuscript

423 to the complete digestion of WT αA-crystallin, confirming the internalization of αA-crystallin
424 recombinant proteins in cells upon its extracellular supplementation (**Figure 5D**).

425 **Effect of αA-crystallin supplementation on neuronal cell viability.** To test the effect of
426 uptake of recombinant αA-crystallins on cell viability under conditions of stress, we sought to
427 establish a dose-response effect of αA-crystallin concentration on R28 cell viability. External
428 supplementation of WT αA-crystallin efficiently prevented serum starvation-induced R28 cell
429 death in a dose-dependent manner (**Figure 6A**) as validated by TUNEL staining. Approximately
430 60% reduction in R28 cell death was observed following incubation with 500 ng/ml WT αA-
431 crystallin, and this dose was selected to assess the relative neuroprotective efficacy of T148D
432 and T148A crystallins in comparison to WT. Figure 5B summarizes the relative efficacies of 500
433 ng/ml WT, T148D, and T148A crystallins in promoting R28 cell survival in response to serum
434 starvation-induced apoptotic stress. Compared to control, incubation with 500 ng/ml T148D
435 crystallin resulted in ~ 85% increased cell viability in comparison to WT (~ 30%). Incubation with
436 500 ng/ml T148A did not promote R28 cell viability, further validating the key role of
437 phosphorylation of αA-crystallin on T148 for its neuroprotective function (**Figure 6B**).

438 To confirm the neuroprotective efficacy of recombinant αA-crystallins in promoting neuronal cell
439 survival, we further tested the ability of the recombinant protein supplementation on the survival
440 of primary retinal ganglion cells (RGCs) under "diabetes-like" conditions. As to avoid potential
441 complications due to induction of endogenous αA-crystallin, RGCs were also isolated from the
442 retinas of αA-crystallin knockout mice, and the purity of the RGC preparation was assessed by
443 staining for neuronal cell-specific markers (**Figures 7A-C**). RGCs cell death under "diabetes-
444 like" conditions was then analyzed by TUNEL and RBPMS co-staining. Consistent with the
445 effect seen in differentiated R28 cells, supplementation with 500 ng/ml of WT or T148D αA-
446 crystallins were highly protective of RGC cells exposed to metabolic stress (**Figure 7D & E**).
447 Also similar to what was observed in R28 cells, co-incubation with T148D was slightly more

protective than WT while T148A crystallin completely failed to prevent cell death, emphasizing an inherent role of T148 phosphorylation on the neuroprotective efficacy of αA-crystallin.

Discussion:

Our present study has shown that primary Müller glial cells can secrete αA-crystallin and that secreted αA-crystallin presents with significant neuroprotective abilities for retinal neuronal cells exposed to metabolic stresses. Supportive of a paracrine function of the secreted protein and therapeutic potential for αA-crystallin recombinant proteins was the demonstration of its increased uptake in stressed retinal neurons. Furthermore, analysis of the biochemical and biophysical properties of these recombinant proteins revealed an increased chaperone activity, smaller oligomer assembly, and an increased solubility of the T148D αA-phosphomimetic, consistent with its enhanced protective effect. Overall, our study shows that supplemented αA-crystallin recombinant proteins are neuroprotective for primary retinal neurons exposed to metabolic stress and that αA-crystallin T148D phosphomimetic mutant presents with enhanced therapeutic ability.

Müller glia has been shown to release trophic factors which regulate the various aspects of retinal neuronal circuitry during the process of synaptogenesis, differentiation, neuroprotection, and survival of photoreceptors and RGCs in the retina (de Melo Reis et al., 2008). Müller glial cells, astrocytes, and microglia also play an important role in the metabolism, the phagocytosis of neuronal debris, the release of certain neurotransmitters, and the release of trophic factors apart from providing structural support (Vecino et al., 2016). They are also reported to be involved in the inflammation associated with the pathophysiology of diabetic retinopathy, with special emphasis on the functional relationships between glial cells and neurons (Rubsam et al., 2018). Müller glial cells are an important source of numerous pro-survival factors under

eNeuro Accepted Manuscript

eNeuro Accepted Manuscript

472 inflammatory conditions to exert neuroprotection, a potentially key point in patients with DR
473 since they have higher levels of both inflammatory cytokines and neurotransmitters in their
474 vitreous (Boss et al., 2017).

475 More recently, it also has been observed that non-toxin-induced Müller cell ablation is
476 detrimental for neurons further supporting their necessity for neuronal viability (Fu et al., 2015).
477 Stem cell-derived RGC-like cells survival was substantially enhanced when co-cultured with
478 adult Müller cells or supplemented with Müller cell-conditioned media and significantly increased
479 their neurite length (Pereiro et al., 2020). Confluent retinal Müller glial cell substrates and its
480 conditioned medium were also reported to significantly increase the survival of cultured porcine
481 RGCs (Garcia et al., 2002). Our current study has also demonstrated that retinal Müller glial
482 cells were able to secrete αA-crystallin, and incubation of either R28 retinal neuronal cells or
483 primary αA-crystallin knockout (AKO) mouse RGCs with the conditioned media resulted in a
484 significant decrease in the cell death induced by metabolic stress. Our study further confirmed
485 the importance of T148 phosphorylation in the neuroprotective function of αA-crystallin as
486 evidenced by the greater protection of retinal neurons by the phosphomimetic mutant
487 conditioned media, while the non-phosphorylatable mutant conditioned media had no effect.

488 The effect of phosphorylation on the structure and function of α-crystallin has largely been
489 studied for αB-crystallin, owing to its ubiquitous distribution and upregulation under stress and
490 disease conditions. Studies investigating chaperone and anti-apoptotic activity of
491 phosphorylated αB-crystallin mostly support a pro-chaperone and anti-apoptotic enhancer role
492 of this phosphorylation under various cellular stresses while underlying a more complex function
493 during development and cancer (Morrison et al., 2003) (Jeong et al., 2012) (Lee et al., 2016). In
494 the meantime, the effect of phosphorylation on the chaperone function and the anti-apoptotic
495 activity of αA-crystallin have evaded diligent investigation.

eNeuro Accepted Manuscript

496 Takemoto et al. first reported an increase in the phosphorylation of αA-crystallin on S122 from
497 donor lens tissue in an age-dependent fashion (Takemoto, 1996). 2D gel electrophoresis on
498 lens tissue of 14-week C57BL6 mice identified T148 in addition to S122 as sites of
499 phosphorylation on αA-crystallin (Reddy et al., 2006). A recent study from our lab was the first to
500 identify T148 phosphorylation *in vivo* from retinal tissue samples from human donors (Ruebsam
501 et al., 2018). The modification was dramatically reduced in donor samples with diabetes,
502 suggesting an inherent role for T148 phosphorylation of αA-crystallin in the pathophysiology of
503 diabetic retinopathy (DR). Overexpression of the αA-crystallin phosphomimetic T148D conferred
504 protection to R28 neuronal cells to serum starvation-induced apoptosis over its non-
505 phosphorylatable analog T148A. The current study, therefore, investigated the structural and
506 functional consequences of T148 phosphorylation on αA-crystallin.

507 Mutations in αA-crystallin have been shown to influence its chaperone activity. Recombinant
508 αA-T148D crystallin exhibited maximal efficiency in preventing EDTA-induced aggregation of
509 Alcohol dehydrogenase over wild-type and T148A crystallin. In conjunction with the observed
510 cytoprotective effect observed in the earlier study, it shows that phosphorylation of T148
511 enhances the chaperone function and the associated anti-apoptotic function of retinal αA-
512 crystallin. Both α-Crystallin proteins have been shown to associate into large oligomeric
513 structures with molar masses ranging from 400-700 kDa. Our study has shown that
514 phosphorylation of αA-crystallin was directly influencing the oligomeric assembly of αA-crystallin
515 *in vitro*. Native gel analysis of recombinant αA-crystallins suggests a change in the
516 polydispersity profile of T148D crystallin, which showed an increased predisposition to form
517 smaller oligomeric assemblies when compared to the wild type and T148A αA-crystallin. Since
518 the chaperone activity of α-crystallin has been shown to be modulated by hydrophobic 'patches'
519 distributed along with its monomeric structure (Datta and Rao, 1999; Rao et al., 1998). The
520 observed oligomeric shift in our present study could translate into a higher number of smaller

eNeuro Accepted Manuscript

521 oligomers exerting their chaperone action. Studies have also demonstrated that exposure of
522 hydrophobic residues by structural modification facilitates chaperoning in α-crystallin proteins
523 whereas the flexible carboxy-terminal extension also contributes to the chaperone activity by
524 enhancing the solubility (MacRae, 2000; Ruebsam *et al.*, 2018). The change in oligomeric
525 profile was less pronounced for T148A crystallin, which was to be expected, as the recombinant
526 WT crystallin protein used in this experiment was similarly unphosphorylated. However, this
527 difference may become more pronounced in the cellular environment as WT αA-crystallin
528 becomes phosphorylated and explains the lack of protective ability of T148A recombinant
529 proteins *in vitro.*

530 αA-crystallin was originally described as an endogenous neuroprotective factor in retinal
531 neurons, as exhibited in over-expression-based studies in hypoxic stress, or glaucomatous and
532 other optic neuropathies (MacRae, 2000). Several studies have also demonstrated that αA-
533 crystallin enhanced endogenous expression has potential as the therapeutic strategy to protect
534 and rescue neurons from degeneration associated with metabolic or hypoxic stress (MacRae,
535 2000; Ying et al., 2014). Similarly, exogenous supplementation of αA-crystallin via intravitreal
536 injections was associated with significantly decreased levels of GFAP in both the retina and the
537 crush site following the 3rd day of optic nerve crush injury and induced astrocytes architecture
538 remodeling at the crush site (Piri *et al.*, 2016). In the increased intraocular pressure model,
539 intravitreal injection of αB-crystallin was also able to increase RGCs survival and function, as
540 measured by functional photopic electroretinogram, retinal nerve fiber layer thickness, and RGC
541 counts (Shao et al., 2016). Another study has reported the enhanced rate of survival in the
542 axotomized axons beyond the crush site after a single intravitreal administration of α-crystallin
543 at the time of axotomy (Anders et al., 2017). Together with these previous reports, the present
544 study strongly supports the protective potential of functionally enhanced αA-crystallin
545 recombinant proteins against neurodegeneration.

546 **Conclusion:**

547 In conclusion, our study demonstrates for the first time that the exogenous supplementation of
548 αA-crystallin, especially its functionally enhanced mutant, promotes retinal cell survival under
549 metabolic stress. Altogether, our data show that αA-crystallin recombinant proteins present a
550 strong potential to reduce neuronal cell death during acute stresses and that its T148D
551 phosphomimetic mutant form could be an interesting option in chronic diseases such as
552 diabetes, due to its improved biochemical properties and enhanced functionality. *In vivo* studies,
553 including in diabetes models are now essential to further demonstrate the potential of this
554 approach and validate the neuroprotective effect of functionally enhanced αA-crystallin
555 recombinant proteins. These studies will also be key in characterizing the mechanisms of action
556 of αA-crystallin *in vivo* in order to unveil αA-crystallin specific involvement in the regulation of
557 neurosurvival and neuroinflammation.

558 **Acknowledgment:** This research was supported by National Eye Institute (EY020895), NIH
559 P30EY007003 (Core Grant for Vision Research at the University of Michigan), and NIH
560 P30DK020572 (Michigan Diabetes Research Center) as well as the Lichter Award, Research to
561 Prevent Blindness (RPB).

562 **Author Contributions:** Conceptualization, Patrice Fort; Data curation, Madhu Nath, Ashutosh
563 Phadte, Zachary B. Sluzala, Yang Shan and Angela Myers; Formal analysis, Madhu Nath,
564 Ashutosh Phadte, Zachary B. Sluzala, Yang Shan and Patrice Fort; Funding acquisition, Patrice
565 Fort; Investigation, Madhu Nath, Zachary B. Sluzala, Ashutosh Phadte and Yang Shan;
566 Methodology, Madhu Nath, Zachary B. Sluzala, Ashutosh Phadte and Yang Shan; Project
567 administration, Patrice Fort; Resources, Angela Myers and Patrice Fort; Software, Madhu Nath,
568 Zachary B. Sluzala, Ashutosh Phadte and Yang Shan; Supervision, Patrice Fort; Writing –
569 original draft, Ashutosh Phadte, Madhu Nath, Zachary B. Sluzala and Patrice Fort; Writing –

eNeuro Accepted Manuscript

eNeuro Accepted Manuscript

570 review & editing, Ashutosh Phadte, Madhu Nath, Zachary B. Sluzala, Yang Shan, Angela Myers
571 and Patrice Fort.

572 **Institutional Review Board Statement:** All experiments were conducted following the
573 Association for Research in Vision and Ophthalmology Resolution on the Care and Use of
574 Laboratory Animals and approved by the Institutional Animal Care and Use Committee of the
575 University of Michigan (Protocol No: PRO-00009143 approved 7/9/2019).

576 **Informed Consent Statement:** Not applicable.

577 **Data Availability Statement:** Data generated is included within the manuscript.

578

579 **Figure Legends**

580 **Figure 1. Expression and secretion of αA-crystallins by Müller cells.** αA-crystallin (CRYAA)
581 expression was observed in the cell lysates and the concentrated growth (conditioned) media.
582 (**A)** Rat retinal Müller (rMC-1) cells and (**B)** primary Müller cells isolated from αA-crystallin
583 knockout (KO) mice were transfected with either empty vector (EV), wild type αA-crystallin (WT),
584 αA-crystallin phosphomimetic (T148D), and the non-phosphorylatable form of αA-crystallin
585 (T148A). 24 hours post-transfection, cells were either exposed to normal media (DMEM-NG +
586 10% FBS), serum starvation (DMEM-NG No FBS), or diabetic-like stress (DMEM-NG + 20 mM
587 glucose +100ng/ml TNFα) for 4 hours.

588 **Figure 2: MGC secreted αA-crystallin promotes neuronal cell survival under stress.** The
589 relative viability of rat retinal neuronal (R28) cells under **(A)** serum starvation stress and **(B)**
590 "Diabetes-like" condition, following supplementation of 'conditioned' media from MGCs
591 overexpressing αA-crystallin. (*$P \leq 0.05$), (**$P \leq 0.01$), (***$P \leq 0.001$), significantly different from
592 respective EV-transfected cells. Representative endpoint statistics result of DNA fragmentation
593 ELISA from three replicates, with relative significance determined by 1-way ANOVA followed by
594 the Tukey post-hoc tests test. Immunoblotting analyses reveal a similar expression pattern of
595 WT, T148A, and T148D crystallins in comparison to EV control under **(C)** serum starvation
596 stress and **(D)** "Diabetes-like" condition. **(E)** The relative viability of primary, αA-crystallin
597 knockout (AKO) mouse retinal ganglion cells (RGC) under basal and stress conditions following

supplementation of 'conditioned media' (CM) from MGCs overexpressing αA-crystallin. Representative endpoint statistics result of TUNEL from 3-4 fields from three coverslips per condition of three replicates, with relative significance determined by 1-way ANOVA followed by Tukey post-hoc tests. The data was expressed as mean ± SD and statistically significant differences are reported. (**P ≤ 0.01), (***P ≤ 0.001), (****P ≤ 0.0001), significantly different from respective EV-transfected cells.

Figure 3. Characterization of recombinant αA-crystallins. (**A**) BL21 purified αA-crystallins were analyzed for purity using SDS page (top panel) and western blot (bottom panel), respectively. (**B)** Triton X-114 treatment of purified αA-crystallins drastically reduces their relative endotoxin content in comparison to non-treated controls. 500 ng of each of the purified proteins was subjected to endotoxin estimation using the LAL assay kit. (**C)** Chaperone assays with ADH show a αA-crystallin concentration-dependent decrease in ADH aggregation, monitored as relative absorbance at 360 nm. The range of αA-crystallin concentrations used is depicted in the legend**. (D)** *In vitro* chaperone activity assays reveal an enhanced chaperone function of T148D crystallin over αA-WT (n=3). The data are represented as mean ± SD and statistically significant differences are reported. (**P ≤ 0.01), (***P ≤ 0.001), (****P ≤ 0.0001), significantly different from respective EV-transfected cells.

Figure 4. Phosphomimetic and non-phosphorylatable mutants of αA-crystallin exhibit differences in stress-induced solubility and oligomeric profile. (A) Representative blot showing relative amounts of soluble (S) and insoluble (I) αA-crystallin after 24 hours of serum deprivation. (**B)** Solubility differences are expressed as a ratio of insoluble αA-crystallin to total αA-crystallin for each condition, normalized to WT. Data are represented as mean ± S.D. Statistical comparisons between groups were calculated by One-Way ANOVA followed by Tukey post-hoc tests (**p<0.01). (**C)** Representative Native gel showing the oligomeric profiles of WT, T148D and T148A αA-crystallin**. (D).** Graphical representation of oligomeric profiles of the native gels (representative of 3 independent experiments). Median oligomer size for each recombinant protein is shown, rounded to the nearest kilodalton.

Figure 5. Selective uptake of recombinant αA-crystallins by R28 cells. All recombinant proteins were supplemented at a concentration of 500 ng/ml. (**A)** Time dependent uptake of recombinant αA-crystallins by R28 cells under serum starvation induced metabolic stress. Uptake of αA-crystallins in R28 cells was dependent on the presence of serum (**B)** and specificity of induced "diabetes-like" conditions **(C)** as mimicked by supplementation of DMEM-NG ± 10% FBS ± 1% BSA and DMEM-HG (25mM) + 10 % FBS ± 100 ng/ml TNFα respectively.

eNeuro Accepted Manuscript

631 (D) Supplemented recombinant αA-crystallins were internalized in the R28 cells as assessed by
632 Proteinase K susceptibility assay.

633 **Figure 6. Effect of αA-crystallin supplementation on R28 cell viability under stress.** All
634 proteins were supplemented to R28 cells in DMEM-NG ± 10% FBS. Following treatment, cell
635 viability was assessed by TUNEL staining. (A) Supplementation of WT suppresses serum
636 starvation induced R28 cell death in a dose dependent manner. (B) T148D crystallin
637 supplementation efficiently prevents R28 cell death under serum starvation induced metabolic
638 stress compared to WT and T148A. Data are representative of four fields from three coverslips
639 per condition and are represented as mean ± S.D. from (***: $p \leq 0.0005$), (****: $p \leq 0.000005$),
640 significantly different from respective EV.

641 **Figure 7. Exogenous αA-crystallin protects primary mice retinal ganglion cells under**
642 **stress.** (A) Seven days post seeding, the RGCs show prominent neural processes. (B)
643 Immunofluorescence analyses highlight prominent staining for neuron-specific βIII-tubulin (B,
644 red), (C) neurofilament (NF-H, green), and RBPMS (red). (D) Vehicle control (VC), Recombinant
645 wild type αA-crystallin (WT), αA-crystallin phosphomimetic (T148D), and the non-
646 phosphorylatable form of αA-crystallin (T148A) were supplemented to RGCs at a 500 ng/ml
647 concentration and incubated for 8 hours with 25 mM D-glucose (HG) and 100 ng/ml TNFα for 8
648 hours. Cells incubated with 5mM glucose (NG) served as an experimental control. RGC survival
649 under stress was assessed by TUNEL staining (green), and cells were later stained for RBPMS
650 (red). (E) Statistical analyses of RGC viability following exposure to stress. Percentage of
651 apoptotic cells (TUNEL positive) in all RGCs (RBPMS positive) were analyzed. Data are
652 represented as mean ± S.D. Statistical comparisons between groups were calculated by One-
653 Way ANOVA followed by Tukey post-hoc tests. (**$P \leq 0.01$), (***$P \leq 0.001$), (****$P \leq 0.0001$),
654 significantly different from respective EV-transfected cells.

655

656

eNeuro Accepted Manuscript

eNeuro Accepted Manuscript

657 **References**

658 Anders, F., Liu, A., Mann, C., Teister, J., Lauzi, J., Thanos, S., Grus, F.H., Pfeiffer, N., and Prokosch, V.
659 (2017). The Small Heat Shock Protein alpha-Crystallin B Shows Neuroprotective Properties in a
660 Glaucoma Animal Model. Int J Mol Sci *18*. 10.3390/ijms18112418.
661 Baba, T., Oshitari, T., and Yamamoto, S. (2015). Level of vitreous alpha-B crystallin in eyes with
662 rhegmatogenous retinal detachment. Graefes Arch Clin Exp Ophthalmol *253*, 1251-1254.
663 10.1007/s00417-014-2815-z.
664 Boss, J.D., Singh, P.K., Pandya, H.K., Tosi, J., Kim, C., Tewari, A., Juzych, M.S., Abrams, G.W., and Kumar,
665 A. (2017). Assessment of Neurotrophins and Inflammatory Mediators in Vitreous of Patients With
666 Diabetic Retinopathy. Invest Ophthalmol Vis Sci *58*, 5594-5603. 10.1167/iovs.17-21973.
667 Brady, J.P., Garland, D., Duglas-Tabor, Y., Robison, W.G., Jr., Groome, A., and Wawrousek, E.F. (1997).
668 Targeted disruption of the mouse alpha A-crystallin gene induces cataract and cytoplasmic inclusion
669 bodies containing the small heat shock protein alpha B-crystallin. Proc Natl Acad Sci U S A *94*, 884-889.
670 Christopher, K.L., Pedler, M.G., Shieh, B., Ammar, D.A., Petrash, J.M., and Mueller, N.H. (2014). Alpha-
671 crystallin-mediated protection of lens cells against heat and oxidative stress-induced cell death. Biochim
672 Biophys Acta *1843*, 309-315. 10.1016/j.bbamcr.2013.11.010.
673 Datta, S.A., and Rao, C.M. (1999). Differential temperature-dependent chaperone-like activity of alphaA-
674 and alphaB-crystallin homoaggregates. J Biol Chem *274*, 34773-34778. 10.1074/jbc.274.49.34773.
675 de Melo Reis, R.A., Ventura, A.L., Schitine, C.S., de Mello, M.C., and de Mello, F.G. (2008). Muller glia as
676 an active compartment modulating nervous activity in the vertebrate retina: neurotransmitters and
677 trophic factors. Neurochem Res *33*, 1466-1474. 10.1007/s11064-008-9604-1.
678 Dubin, R.A., Gopal-Srivastava, R., Wawrousek, E.F., and Piatigorsky, J. (1991). Expression of the murine
679 alpha B-crystallin gene in lens and skeletal muscle: identification of a muscle-preferred enhancer. Mol
680 Cell Biol *11*, 4340-4349. 10.1128/mcb.11.9.4340-4349.1991.
681 Dulle, J.E., and Fort, P.E. (2016). Crystallins and neuroinflammation: The glial side of the story. Biochim
682 Biophys Acta *1860*, 278-286. 10.1016/j.bbagen.2015.05.023.
683 Fort, P.E., Freeman, W.M., Losiewicz, M.K., Singh, R.S., and Gardner, T.W. (2009). The retinal proteome
684 in experimental diabetic retinopathy: up-regulation of crystallins and reversal by systemic and periocular
685 insulin. Mol Cell Proteomics *8*, 767-779. 10.1074/mcp.M800326-MCP200.
686 Fu, S., Dong, S., Zhu, M., Sherry, D.M., Wang, C., You, Z., Haigh, J.J., and Le, Y.Z. (2015). Muller Glia Are a
687 Major Cellular Source of Survival Signals for Retinal Neurons in Diabetes. Diabetes *64*, 3554-3563.
688 10.2337/db15-0180.
689 Garcia, M., Forster, V., Hicks, D., and Vecino, E. (2002). Effects of muller glia on cell survival and
690 neuritogenesis in adult porcine retina in vitro. Invest Ophthalmol Vis Sci *43*, 3735-3743.
691 Ghosh, K.S., and Chauhan, P. (2019). Crystallins and Their Complexes. Subcell Biochem *93*, 439-460.
692 10.1007/978-3-030-28151-9_14.
693 Heinig, N., Schumann, U., Calzia, D., Panfoli, I., Ader, M., Schmidt, M.H.H., Funk, R.H.W., and Roehlecke,
694 C. (2020). Photobiomodulation Mediates Neuroprotection against Blue Light Induced Retinal
695 Photoreceptor Degeneration. Int J Mol Sci *21*. 10.3390/ijms21072370.
696 Heise, E.A., Marozas, L.M., Grafton, S.A., Green, K.M., Kirwin, S.J., and Fort, P.E. (2013). Strain-
697 independent increases of crystallin proteins in the retina of type 1 diabetic rats. PLoS One *8*, e82520.
698 10.1371/journal.pone.0082520.
699 Hejtmancik, J.F., Riazuddin, S.A., McGreal, R., Liu, W., Cvekl, A., and Shiels, A. (2015). Lens Biology and
700 Biochemistry. Prog Mol Biol Transl Sci *134*, 169-201. 10.1016/bs.pmbts.2015.04.007.
701 Hicks, D., and Courtois, Y. (1990). The growth and behaviour of rat retinal Muller cells in vitro. 1. An
702 improved method for isolation and culture. Exp Eye Res *51*, 119-129. 10.1016/0014-4835(90)90063-z.

eNeuro Accepted Manuscript

703 Horwitz, J. (1992). Alpha-crystallin can function as a molecular chaperone. Proc Natl Acad Sci U S A *89*,
704 10449-10453. 10.1073/pnas.89.21.10449.
705 Horwitz, J., Bova, M.P., Ding, L.L., Haley, D.A., and Stewart, P.L. (1999). Lens alpha-crystallin: function
706 and structure. Eye (Lond) *13 (Pt 3b)*, 403-408. 10.1038/eye.1999.114.
707 Hua Wang, Y., Wu Wang, D., and Qin Yin, Z. (2020). Synergistic protection of RGCs by olfactory
708 ensheathing cells and alpha-crystallin through regulation of the Akt/BAD Pathway. J Fr Ophtalmol *43*,
709 718-726. 10.1016/j.jfo.2020.02.003.
710 Jeong, W.J., Rho, J.H., Yoon, Y.G., Yoo, S.H., Jeong, N.Y., Ryu, W.Y., Ahn, H.B., Park, W.C., Rho, S.H., Yoon,
711 H.S., et al. (2012). Cytoplasmic and nuclear anti-apoptotic roles of alphaB-crystallin in retinal pigment
712 epithelial cells. PLoS One *7*, e45754. 10.1371/journal.pone.0045754.
713 Kannan, R., Sreekumar, P.G., and Hinton, D.R. (2016). Alpha crystallins in the retinal pigment epithelium
714 and implications for the pathogenesis and treatment of age-related macular degeneration. Biochim
715 Biophys Acta *1860*, 258-268. 10.1016/j.bbagen.2015.05.016.
716 Kase, S., Meghpara, B.B., Ishida, S., and Rao, N.A. (2012). Expression of alpha-crystallin in the retina of
717 human sympathetic ophthalmia. Mol Med Rep *5*, 395-399. 10.3892/mmr.2011.653.
718 Kim, Y.H., Choi, M.Y., Kim, Y.S., Han, J.M., Lee, J.H., Park, C.H., Kang, S.S., Choi, W.S., and Cho, G.J. (2007).
719 Protein kinase C delta regulates anti-apoptotic alphaB-crystallin in the retina of type 2 diabetes.
720 Neurobiol Dis *28*, 293-303. 10.1016/j.nbd.2007.07.017.
721 Lee, S.W., Rho, J.H., Lee, S.Y., Yoo, S.H., Kim, H.Y., Chung, W.T., and Yoo, Y.H. (2016). Alpha B-Crystallin
722 Protects Rat Articular Chondrocytes against Casein Kinase II Inhibition-Induced Apoptosis. PLoS One *11*,
723 e0166450. 10.1371/journal.pone.0166450.
724 Liu, J.P., Schlosser, R., Ma, W.Y., Dong, Z., Feng, H., Liu, L., Huang, X.Q., Liu, Y., and Li, D.W. (2004).
725 Human alphaA- and alphaB-crystallins prevent UVA-induced apoptosis through regulation of PKCalpha,
726 RAF/MEK/ERK and AKT signaling pathways. Exp Eye Res *79*, 393-403. 10.1016/j.exer.2004.06.015.
727 Losiewicz, M.K., and Fort, P.E. (2011). Diabetes impairs the neuroprotective properties of retinal alpha-
728 crystallins. Invest Ophthalmol Vis Sci *52*, 5034-5042. iovs.10-6931 [pii]

729 10.1167/iovs.10-6931.
730 MacRae, T.H. (2000). Structure and function of small heat shock/alpha-crystallin proteins: established
731 concepts and emerging ideas. Cell Mol Life Sci *57*, 899-913. 10.1007/pl00000733.
732 Makley, L.N., McMenimen, K.A., DeVree, B.T., Goldman, J.W., McGlasson, B.N., Rajagopal, P., Dunyak,
733 B.M., McQuade, T.J., Thompson, A.D., Sunahara, R., et al. (2015). Pharmacological chaperone for alpha-
734 crystallin partially restores transparency in cataract models. Science *350*, 674-677.
735 10.1126/science.aac9145.
736 Masilamoni, J.G., Jesudason, E.P., Bharathi, S.N., and Jayakumar, R. (2005). The protective effect of
737 alpha-crystallin against acute inflammation in mice. Biochim Biophys Acta *1740*, 411-420.
738 10.1016/j.bbadis.2004.11.002.
739 Morrison, L.E., Hoover, H.E., Thuerauf, D.J., and Glembotski, C.C. (2003). Mimicking phosphorylation of
740 alphaB-crystallin on serine-59 is necessary and sufficient to provide maximal protection of cardiac
741 myocytes from apoptosis. Circ Res *92*, 203-211. 10.1161/01.res.0000052989.83995.a5.
742 Munemasa, Y., Kwong, J.M., Caprioli, J., and Piri, N. (2009). The role of alphaA- and alphaB-crystallins in
743 the survival of retinal ganglion cells after optic nerve axotomy. Invest Ophthalmol Vis Sci *50*, 3869-3875.
744 10.1167/iovs.08-3138.
745 Nath, M., Shan, Y., Myers, A.M., and Fort, P.E. (2021). HspB4/alphaA-Crystallin Modulates
746 Neuroinflammation in the Retina via the Stress-Specific Inflammatory Pathways. J Clin Med *10*.
747 10.3390/jcm10112384.

eNeuro Accepted Manuscript

748 Pasupuleti, N., Matsuyama, S., Voss, O., Doseff, A.I., Song, K., Danielpour, D., and Nagaraj, R.H. (2010).
749 The anti-apoptotic function of human alphaA-crystallin is directly related to its chaperone activity. Cell
750 Death Dis *1*, e31. 10.1038/cddis.2010.3.
751 Pereiro, X., Miltner, A.M., La Torre, A., and Vecino, E. (2020). Effects of Adult Muller Cells and Their
752 Conditioned Media on the Survival of Stem Cell-Derived Retinal Ganglion Cells. Cells *9*.
753 10.3390/cells9081759.
754 Piri, N., Kwong, J.M., and Caprioli, J. (2013). Crystallins in retinal ganglion cell survival and regeneration.
755 Mol Neurobiol *48*, 819-828. 10.1007/s12035-013-8470-2.
756 Piri, N., Kwong, J.M., Gu, L., and Caprioli, J. (2016). Heat shock proteins in the retina: Focus on HSP70
757 and alpha crystallins in ganglion cell survival. Prog Retin Eye Res *52*, 22-46.
758 10.1016/j.preteyeres.2016.03.001.
759 Rao, C.M., Raman, B., Ramakrishna, T., Rajaraman, K., Ghosh, D., Datta, S., Trivedi, V.D., and
760 Sukhaswami, M.B. (1998). Structural perturbation of alpha-crystallin and its chaperone-like activity. Int J
761 Biol Macromol *22*, 271-281. 10.1016/s0141-8130(98)00025-7.
762 Rao, N.A., Saraswathy, S., Wu, G.S., Katselis, G.S., Wawrousek, E.F., and Bhat, S. (2008). Elevated retina-
763 specific expression of the small heat shock protein, alphaA-crystallin, is associated with photoreceptor
764 protection in experimental uveitis. Invest Ophthalmol Vis Sci *49*, 1161-1171. 49/3/1161 [pii]

765 10.1167/iovs.07-1259.
766 Reddy, G.B., Kumar, P.A., and Kumar, M.S. (2006). Chaperone-like activity and hydrophobicity of alpha-
767 crystallin. IUBMB Life *58*, 632-641. 10.1080/15216540601010096.
768 Reddy, V.S., Raghu, G., Reddy, S.S., Pasupulati, A.K., Suryanarayana, P., and Reddy, G.B. (2013).
769 Response of small heat shock proteins in diabetic rat retina. Invest Ophthalmol Vis Sci *54*, 7674-7682.
770 10.1167/iovs.13-12715.
771 Robinson, M.L., and Overbeek, P.A. (1996). Differential expression of alpha A- and alpha B-crystallin
772 during murine ocular development. Invest Ophthalmol Vis Sci *37*, 2276-2284.
773 Rodriguez, A.R., de Sevilla Muller, L.P., and Brecha, N.C. (2014). The RNA binding protein RBPMS is a
774 selective marker of ganglion cells in the mammalian retina. J Comp Neurol *522*, 1411-1443.
775 10.1002/cne.23521.
776 Rubsam, A., Parikh, S., and Fort, P.E. (2018). Role of Inflammation in Diabetic Retinopathy. Int J Mol Sci
777 *19*. 10.3390/ijms19040942.
778 Ruebsam, A., Dulle, J.E., Myers, A.M., Sakrikar, D., Green, K.M., Khan, N.W., Schey, K., and Fort, P.E.
779 (2018). A specific phosphorylation regulates the protective role of alphaA-crystallin in diabetes. JCI
780 Insight *3*. 10.1172/jci.insight.97919.
781 Schmidt, T., Bartelt-Kirbach, B., and Golenhofen, N. (2012). Phosphorylation-dependent subcellular
782 localization of the small heat shock proteins HspB1/Hsp25 and HspB5/alphaB-crystallin in cultured
783 hippocampal neurons. Histochem Cell Biol *138*, 407-418. 10.1007/s00418-012-0964-x.
784 Schneider, C.A., Rasband, W.S., and Eliceiri, K.W. (2012). NIH Image to ImageJ: 25 years of image
785 analysis. Nature Methods *9*, 671-675. 10.1038/nmeth.2089.
786 Shao, W.Y., Liu, X., Gu, X.L., Ying, X., Wu, N., Xu, H.W., and Wang, Y. (2016). Promotion of axon
787 regeneration and inhibition of astrocyte activation by alpha A-crystallin on crushed optic nerve. Int J
788 Ophthalmol *9*, 955-966. 10.18240/ijo.2016.07.04.
789 Shi, Y., Su, C., Wang, J.T., Du, B., Dong, L.J., Liu, A.H., and Li, X.R. (2015). Temporal and spatial changes in
790 VEGF, alphaA- and alphaB-crystallin expression in a mouse model of oxygen-induced retinopathy. Int J
791 Clin Exp Med *8*, 3349-3359.
792 Takemoto, L.J. (1996). Differential phosphorylation of alpha-A crystallin in human lens of different age.
793 Exp Eye Res *62*, 499-504. 10.1006/exer.1996.0060.

eNeuro Accepted Manuscript

794 Teodorowicz, M., Perdijk, O., Verhoek, I., Govers, C., Savelkoul, H.F.J., Tang, Y., Wichers, H., and
795 Broersen, K. (2017). Optimized Triton X-114 assisted lipopolysaccharide (LPS) removal method reveals
796 the immunomodulatory effect of food proteins. PLOS ONE *12*, e0173778.
797 10.1371/journal.pone.0173778.
798 Vecino, E., Rodriguez, F.D., Ruzafa, N., Pereiro, X., and Sharma, S.C. (2016). Glia-neuron interactions in
799 the mammalian retina. Prog Retin Eye Res *51*, 1-40. 10.1016/j.preteyeres.2015.06.003.
800 Wang, Y.H., Wang, D.W., Wu, N., Wang, Y., and Yin, Z.Q. (2011). Alpha-crystallin promotes rat retinal
801 neurite growth on myelin substrates in vitro. Ophthalmic Res *45*, 164-168. 10.1159/000319944.
802 Winzeler, A., and Wang, J.T. (2013). Purification and culture of retinal ganglion cells from rodents. Cold
803 Spring Harb Protoc *2013*, 643-652. 10.1101/pdb.prot074906.
804 Yaung, J., Kannan, R., Wawrousek, E.F., Spee, C., Sreekumar, P.G., and Hinton, D.R. (2008). Exacerbation
805 of retinal degeneration in the absence of alpha crystallins in an in vivo model of chemically induced
806 hypoxia. Exp Eye Res *86*, 355-365. S0014-4835(07)00323-5 [pii]

807 10.1016/j.exer.2007.11.007.
808 Ying, X., Peng, Y., Zhang, J., Wang, X., Wu, N., Zeng, Y., and Wang, Y. (2014). Endogenous alpha-crystallin
809 inhibits expression of caspase-3 induced by hypoxia in retinal neurons. Life Sci *111*, 42-46.
810 10.1016/j.lfs.2014.07.008.
811 Ying, X., Zhang, J., Wang, Y., Wu, N., Wang, Y., and Yew, D.T. (2008). Alpha-crystallin protected axons
812 from optic nerve degeneration after crushing in rats. J Mol Neurosci *35*, 253-258. 10.1007/s12031-007-
813 9010-1.
814 Zhang, J., Liu, J., Wu, J., Li, W., Chen, Z., and Yang, L. (2019). Progression of the role of CRYAB in signaling
815 pathways and cancers. Onco Targets Ther *12*, 4129-4139. 10.2147/OTT.S201799.
816 Zhu, Z., and Reiser, G. (2018). The small heat shock proteins, especially HspB4 and HspB5 are promising
817 protectants in neurodegenerative diseases. Neurochem Int *115*, 69-79. 10.1016/j.neuint.2018.02.006.

818

819

eNeuro Accepted Manuscript

820 Table 1: Primers used for point mutations on T148 corresponding to the phosphomimetic (T148D) and
821 the non-phosphorylatable (T148A) analogue of αA-crystallin.

822

Protein	Primers
T148A	5'-gcatccaggccagcctggatcttgggg-3'
	5'-ccccaagatccaggctggcctggatgc-3'
T148D	5'-gtggcatccaggccatcctggatcttggggcc-3'
	5'-ggccccaagatccaggatggcctggatgccac-3'

823

824

eNeuro Accepted Manuscript

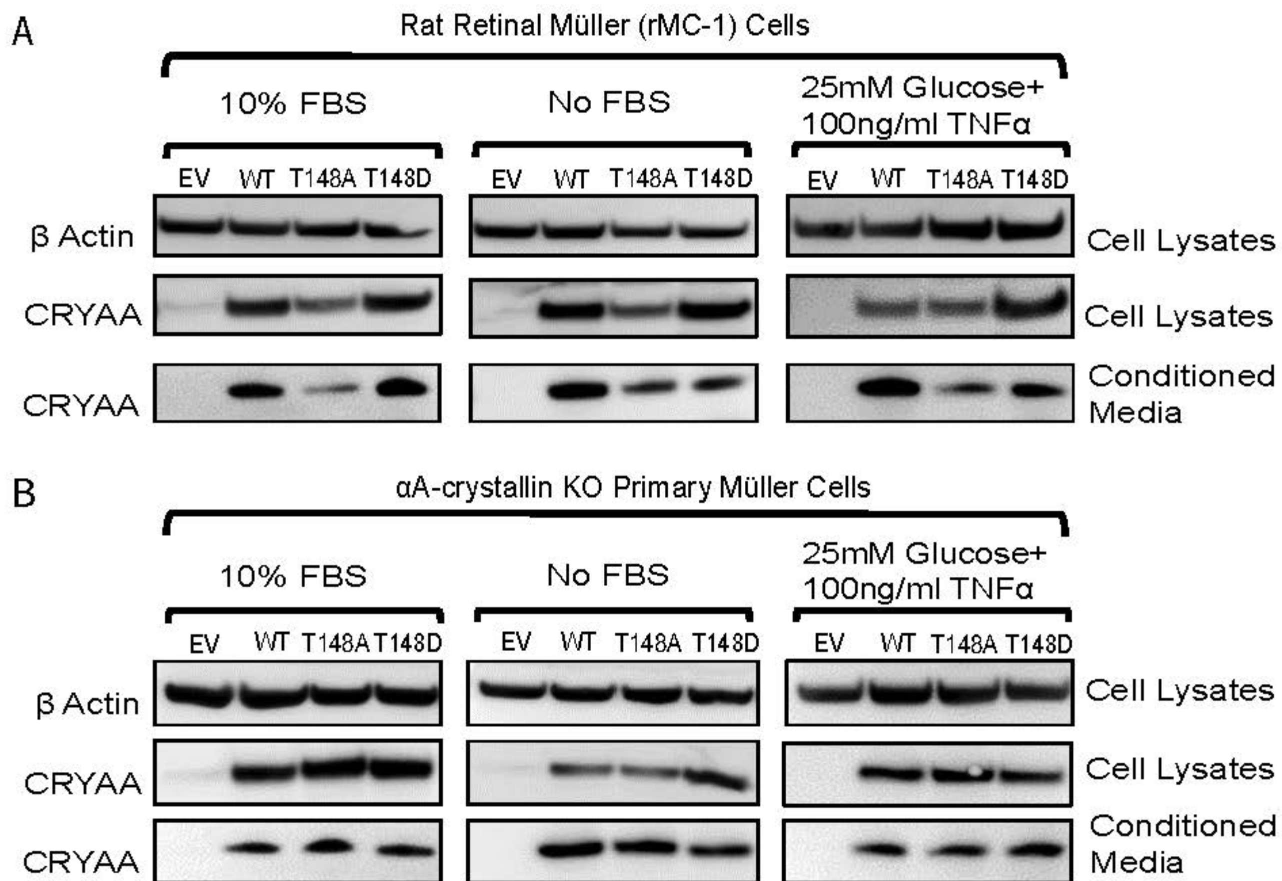

eNeuro Accepted Manuscript

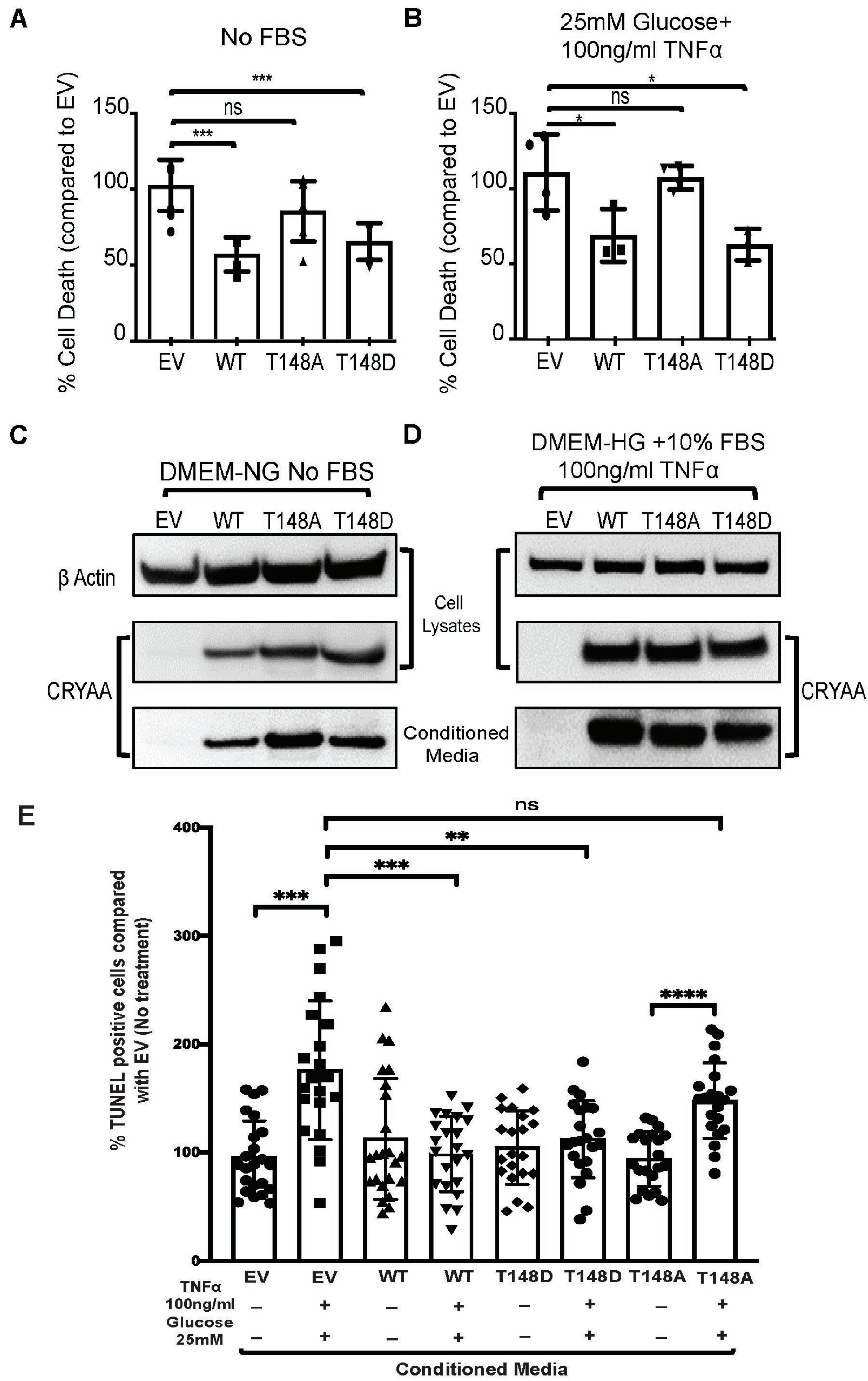

eNeuro Accepted Manuscript

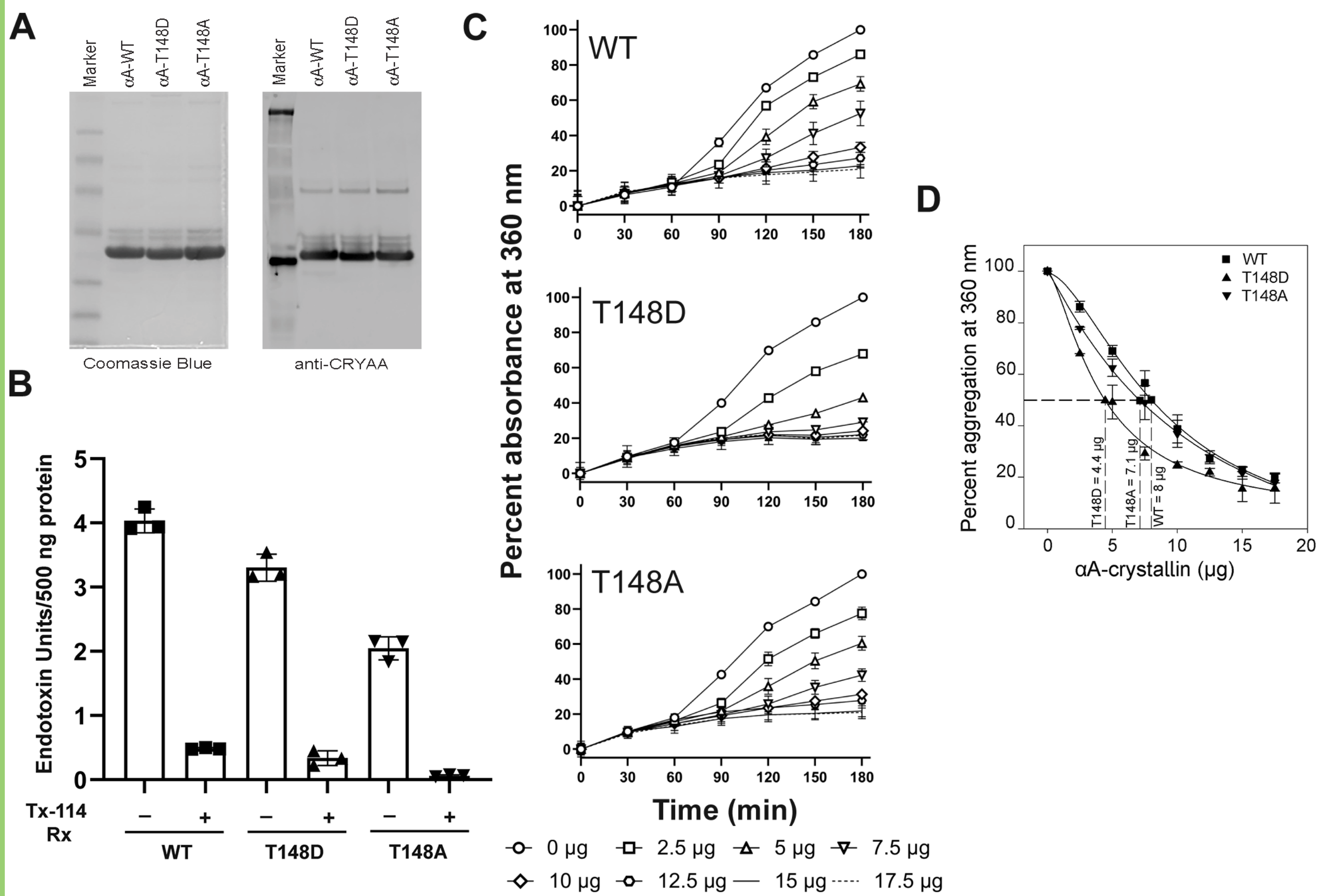

eNeuro Accepted Manuscript

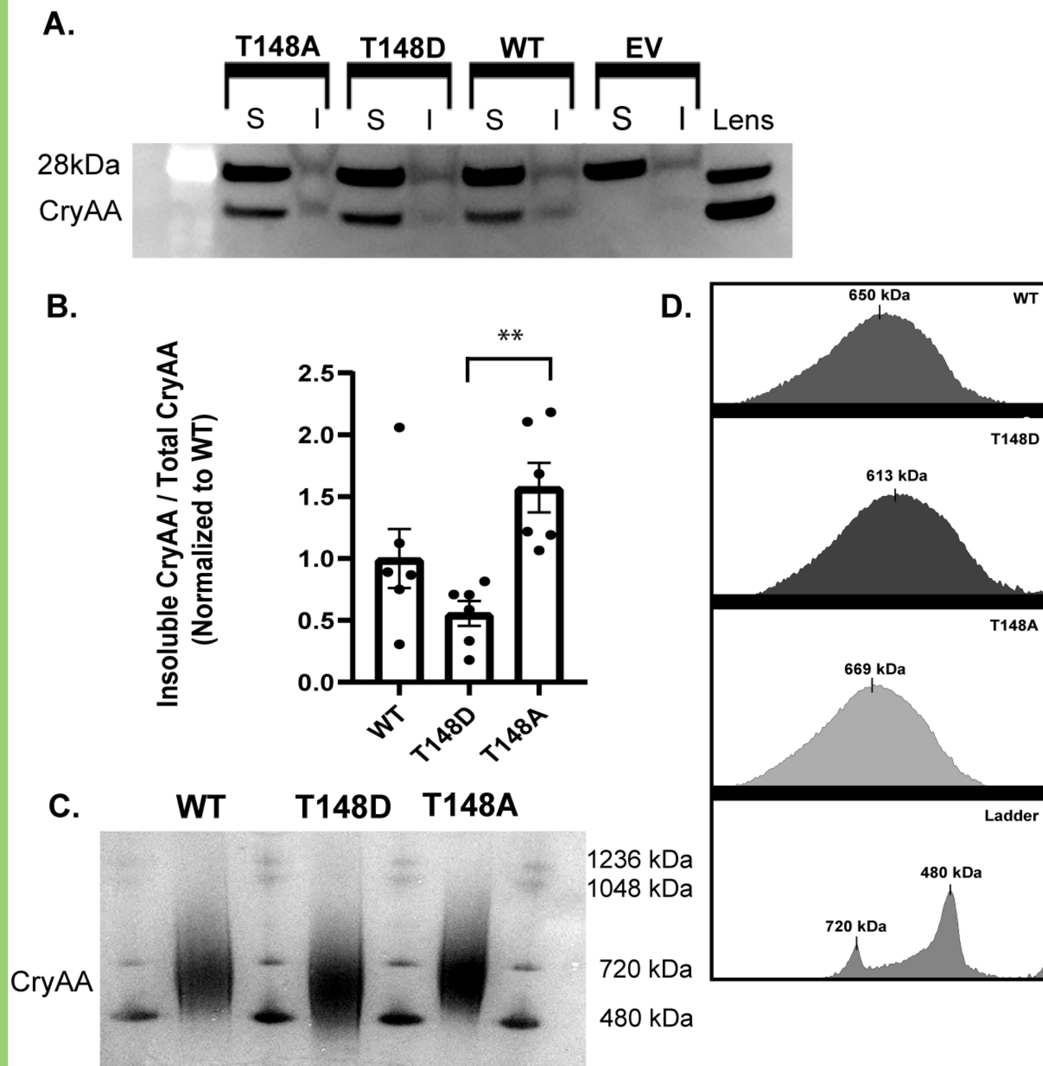

eNeuro Accepted Manuscript

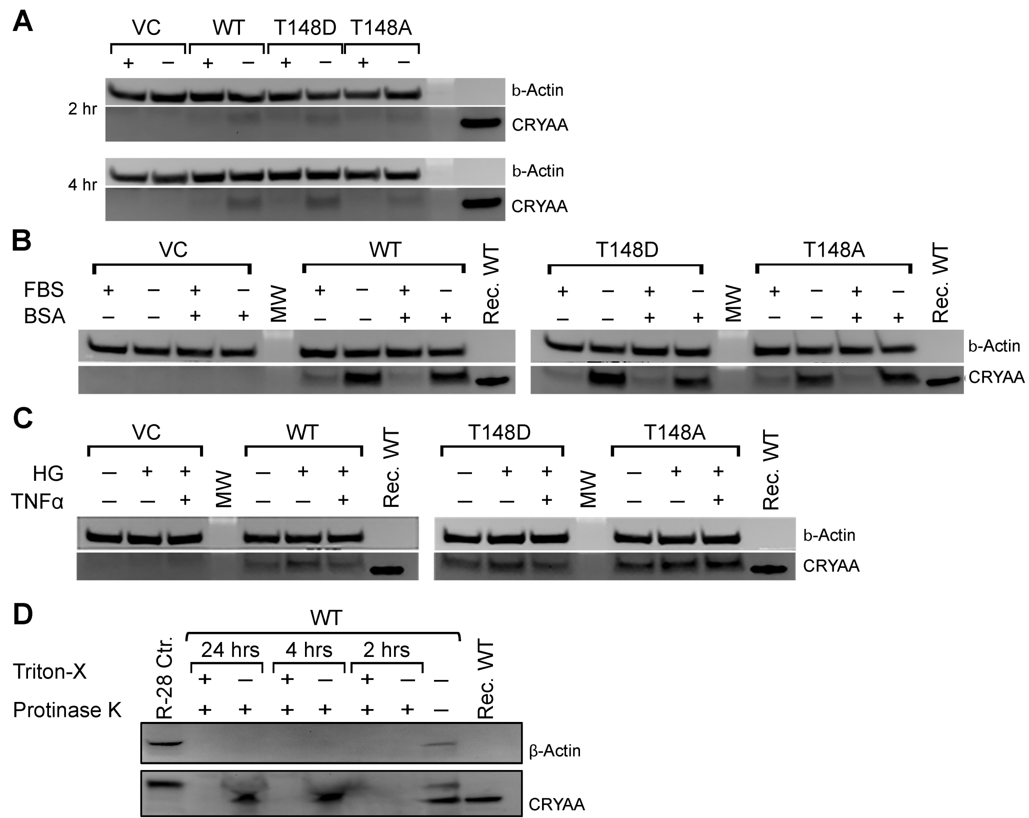

eNeuro Accepted Manuscript

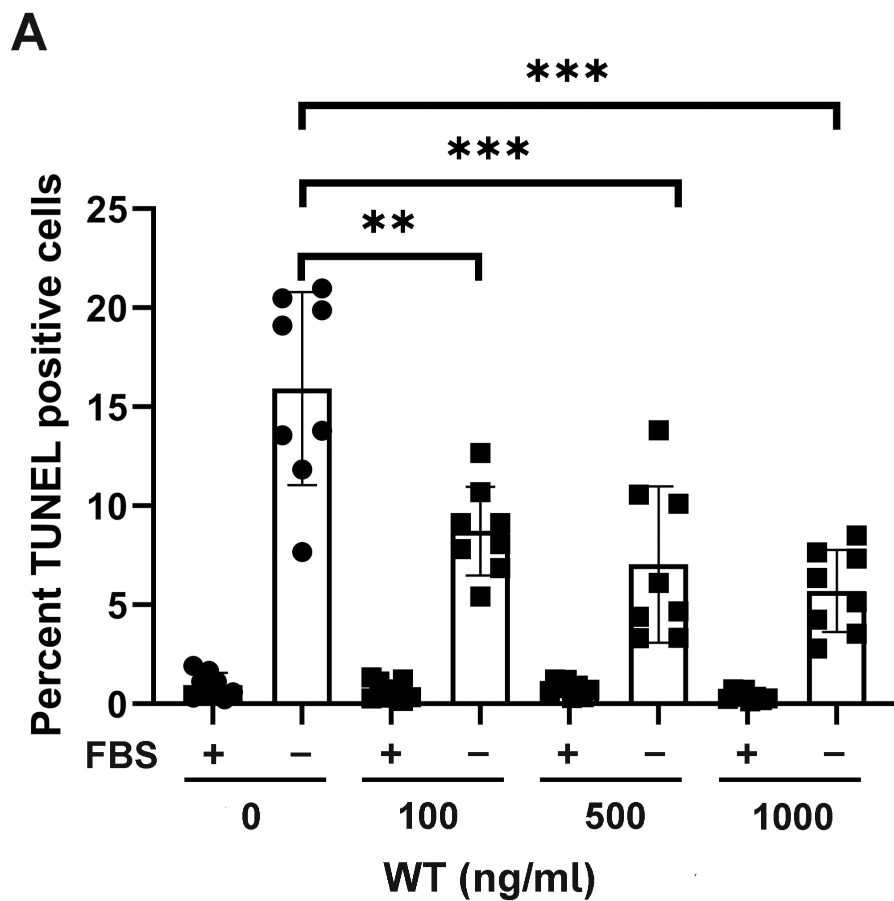

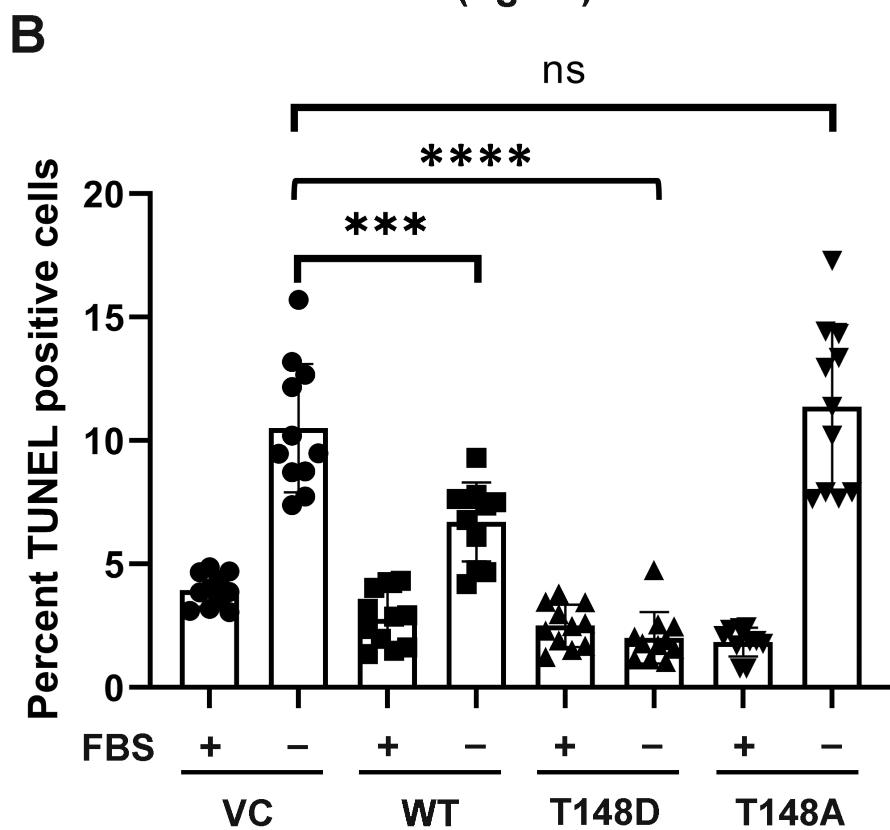

eNeuro Accepted Manuscript